Biochimica et Biophysica Acta 1830 (2013) 4171–4178

Contents lists available at SciVerse ScienceDirect

Biochimica et Biophysica Acta

journal homepage: www.elsevier.com/locate/bbagen

In vivo enzymatic activity of acetylCoA synthetase in skeletal muscle revealed by ^{13}C turnover from hyperpolarized [1-^{13}C]acetate to [1-^{13}C]acetylcarnitine

Jessica A.M. Bastiaansen [a], Tian Cheng [b], Mor Mishkovsky [a,c], João M.N. Duarte [a,c], Arnaud Comment [b,*], Rolf Gruetter [a,c,d]

[a] Laboratory for Functional and Metabolic Imaging, Ecole Polytechnique Fédérale de Lausanne, CH-1015, Lausanne, Switzerland
[b] Institute of Physics of Biological Systems, Ecole Polytechnique Fédérale de Lausanne, CH-1015, Lausanne, Switzerland
[c] Department of Radiology, University of Lausanne, CH-1015, Lausanne, Switzerland
[d] Department of Radiology, Geneva University Hospital and Faculty of Medicine, University of Geneva, CH-1211, Genève 4, Switzerland

ARTICLE INFO

Article history:
Received 13 December 2012
Received in revised form 20 March 2013
Accepted 22 March 2013
Available online 29 March 2013

Keywords:
Acetate
Acetylcarnitine
AcetylCoA synthetase
Skeletal muscle
Hyperpolarization
Magnetic resonance

ABSTRACT

Background: Acetate metabolism in skeletal muscle is regulated by acetylCoA synthetase (ACS). The main function of ACS is to provide cells with acetylCoA, a key molecule for numerous metabolic pathways including fatty acid and cholesterol synthesis and the Krebs cycle.
Methods: Hyperpolarized [1-^{13}C]acetate prepared via dissolution dynamic nuclear polarization was injected intravenously at different concentrations into rats. The ^{13}C magnetic resonance signals of [1-^{13}C]acetate and [1-^{13}C]acetylcarnitine were recorded *in vivo* for 1 min. The kinetic rate constants related to the transformation of acetate into acetylcarnitine were deduced from the 3 s time resolution measurements using two approaches, either mathematical modeling or relative metabolite ratios.
Results: Although separated by two biochemical transformations, a kinetic analysis of the ^{13}C label flow from [1-^{13}C]acetate to [1-^{13}C]acetylcarnitine led to a unique determination of the activity of ACS. The *in vivo* Michaelis constants for ACS were $K_M = 0.35 \pm 0.13$ mM and $V_{max} = 0.199 \pm 0.031$ μmol/g/min.
Conclusions: The conversion rates from hyperpolarized acetate into acetylcarnitine were quantified *in vivo* and, although separated by two enzymatic reactions, these rates uniquely defined the activity of ACS. The conversion rates associated with ACS were obtained using two analytical approaches, both methods yielding similar results.
General significance: This study demonstrates the feasibility of directly measuring ACS activity *in vivo* and, since the activity of ACS can be affected by various pathological states such as cancer or diabetes, the proposed method could be used to non-invasively probe metabolic signatures of ACS in diseased tissue.

1. Introduction

Acetate plays an important role in human and rodent energy metabolism and it is readily taken up by skeletal muscle [1–3] (see Fig. 1). Acetate is a pyruvate dehydrogenase (PDH) independent acetylator of tissue carnitine and free coenzyme A (CoA) [1] and is converted into acetylCoA via a reaction catalyzed by the enzyme acetylCoA synthetase (ACS). The main function of ACS is to provide the cell with acetylCoA, a key molecule for numerous metabolic pathways including fatty acid and cholesterol synthesis and the tricarboxylic acid (TCA) cycle. ACS has been previously shown to be the rate limiting enzyme in the metabolism of acetate [4,5]. Pathological and substrate changes have an effect on the activity of ACS, which has been reported to be turned off faster than other CoA dependent enzymes during free CoA decrease. [6]. Its activity increases together with insulin in response to a carbohydrate-rich diet to induce fatty acid synthesis [7].

Carnitine acetyltransferase (CAT) converts acetylCoA to acetylcarnitine, a reaction which has a well maintained equilibrium [8]. In skeletal muscle, carnitine plays two metabolic roles: on one hand it serves as a shuttle of acetyl groups and long chain fatty acids from the cytosol into mitochondria and thus enabling beta oxidation [9–13]. On the other hand it can act as a buffer for excess acetylCoA when the rate of acetylCoA generation is greater than its entry into the TCA cycle. The general function of CAT is to balance rapid changes in the acetylCoA/CoA ratio in both the cytoplasmic and mitochondrial compartments [11]. In rat skeletal muscle, 98% to 99% of extra acetylCoA produced is buffered by acetylcarnitine [14]. Since the mitochondrial inner membrane is impermeable to acetylCoA, CAT is essential in the metabolism of acetate, as was shown in canine skeletal muscle [15]. After

Abbreviations: CAT, carnitine acetyltransferase; A.CoA, acetyl coenzyme A; ACS, acetylCoA synthetase; TCA, tricarboxylic acid cycle; Ace, acetate; A.Car, acetylcarnitine

* Corresponding author at: Institute of Physics of Biological Systems, LIFMET-IPSB-SB, EPFL, Station 6, CH-1015 Lausanne, Switzerland. Tel.: +41 21 693 7982; fax: +41 21 693 7960.
E-mail address: arnaud.comment@epfl.ch (A. Comment).

0304-4165/$ – see front matter © 2013 Elsevier B.V. All rights reserved.
http://dx.doi.org/10.1016/j.bbagen.2013.03.023

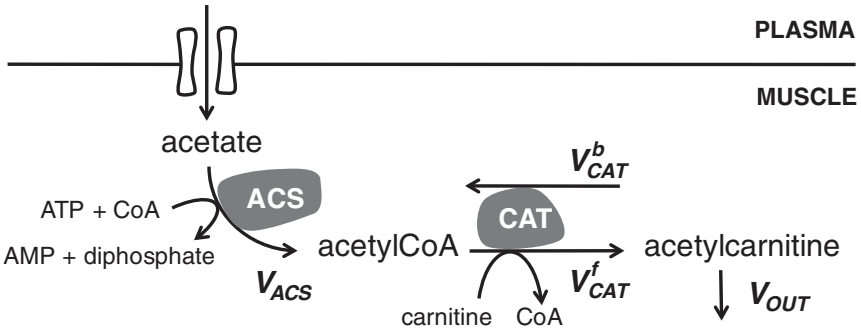

Fig. 1. Schematic representation of the uptake and metabolism of acetate in rat skeletal muscle *in vivo*. Acetate diffusion into the muscle cell is facilitated by a concentration gradient. Via acetylCoA synthetase (ACS), it is transformed to acetylCoA. Carnitine acetyltransferase (CAT) reversibly converts acetylCoA to acetylcarnitine from which there is a flux into the mitochondria (V_{out}).

transformation to acetylcarnitine it traverses the inner mitochondrial membrane via acetylcarnitine translocase (ATL) where a mitochondrial CAT transfers the acetyl group back to CoASH upon which acetylCoA can enter the TCA cycle.

Acetate, being a short chain fatty acid has a typical plasma concentration of 0.2 mM in rats which decreases during fasting and increases in a diabetic state [5]. Its oxidation has been deemed significant since it is rapidly cleared from the blood if injected *in vivo* or generated from precursors such as ethanol in the liver [16]. Acetate uptake by resting skeletal muscle is driven by a concentration gradient and is proportional to the plasma concentration [17,18]. In a single passage of blood, half of the acetate presented to the tissue was removed by the muscle tissue indicating a high affinity for acetate [5]. In contracting skeletal muscle however, acetate oxidation decreased, indicating a shift of substrate preference compared to resting skeletal muscle [19].

To date, most of the information concerning these enzyme activities in rat has however been collected from cell cultures and tissue preparations [5,20]. The ability to measure ACS and CAT activities *in vivo* is expected to provide valuable insight in normal and pathological conditions.

^{13}C magnetic resonance spectroscopy (MRS) is a well-established technique to investigate *in vivo* metabolic processes [21] and it can be coupled with standard MR imaging techniques that gives anatomical information. The advent of dissolution dynamic nuclear polarization (DNP) allows for the measurement of specific metabolic reactions in real-time, thanks to a sensitivity enhancement of several orders of magnitude [22,23], which is now being used in human trials in the investigation of prostate cancer [24].

The incorporation of ^{13}C into acetylcarnitine has been reported after the infusion of hyperpolarized ^{13}C acetate [25] and after the injection of [2-^{13}C]pyruvate [26,27]. The aim of the present study was to elucidate the enzyme kinetics involved in the *in vivo* transformation of acetate to acetylcarnitine in rat skeletal muscle, by extracting quantitative kinetic rate constants from the observed [1-^{13}C] acetylcarnitine labeling dynamics following the infusion of different substrate concentrations of hyperpolarized [1-^{13}C]acetate.

2. Material and methods

All chemicals were purchased from Sigma-Aldrich, Basel, Switzerland. [1-^{13}C]sodium acetate was dissolved in a concentration ranging from 1.0 to 4.5 M in a 1:2 mixture of d_6-EtOD/D_2O containing 33 mM of TEMPO (2,2,6,6-Tetramethyl-1-piperidinyloxy) free radical. 300 μL of the resulting solution was rapidly frozen in liquid nitrogen to form 10 μL beads that were placed in a 5 T custom-designed DNP polarizer [28,29]. The ^{13}C nuclear spins were dynamically polarized at 1.02 ± 0.03 K for 2 h using 30 mW of microwave power at 140.18 GHz. The sample was consecutively rapidly dissolved using 6.0 mL of superheated D_2O and transferred within 2 s to a separator/infusion pump located inside a 9.4 T horizontal bore magnet containing 0.6 mL of phosphate buffered saline and heparin. Subsequently, 1.0 mL of the room-temperature hyperpolarized acetate solution was automatically infused into the animal within 5 s. From *in vitro* measurements performed inside the separator/infusion pump, it was determined that the ^{13}C polarization at the time of injection was 13 ± 2% [30]. No physiological changes were observed during the injection.

All animal experiments were conducted according to federal ethical guidelines and were approved by the local regulatory body. Male Sprague Dawley® rats (275–325 g) were anesthetized with 1.5% isoflurane in oxygen (n = 19). A catheter was placed into the femoral vein for intravenous delivery of the hyperpolarized acetate solution. The respiration rate and temperature were monitored and maintained during the experiment.

All experiments were performed with a Direct Drive spectrometer (Agilent, Palo Alto, CA, USA) interfaced to an actively shielded 9.4 T magnet with a 31 cm horizontal bore (Magnex Scientific, Abingdon, UK). A home-built ^{1}H/^{13}C probe consisting of a pair of 10 mm diameter ^{1}H surface coils in quadrature mode and a 10 mm diameter ^{13}C surface coil was placed over the hind leg of the rat to selectively excite and detect skeletal muscle tissue, more specifically, the gastrocnemius muscles. A hollow glass sphere with a 3 mm inner diameter (Wilmad-LabGlass, NJ, USA) was filled with a 1 M [1-^{13}C]glucose solution and used to adjust the pulse power and set the reference frequency. Once the animal was positioned inside the magnet, ten axial 1 mm thick slices were acquired using a gradient echo sequence (TR = 50 ms, TE = 3 ms, field of view = 30 × 30 mm^2, matrix = 128 × 128, flip angle = 30°) from which the volume of interest was selected. The static magnetic field was homogenized in a 600 μL (6 × 10 × 10 mm^3) voxel to reduce the localized proton line width to 20 Hz using the FASTESTMAP shimming protocol [31]. Series of single-pulse ^{13}C acquisitions were sequentially recorded starting 12 s after dissolution using 30° adiabatic RF pulses (BIR4) applied every 3 s with ^{1}H decoupling during acquisition (WALTZ). The adiabatic pulse offset and power was set such as to ensure a homogeneous 30° excitation of substrate and metabolite resonances in the entire volume of interest. At the end of each *in vivo* experiment, 200 μL of the residual solution was collected from the infusion pump and the [1-^{13}C]acetate concentration was measured in a high-resolution 400 MHz NMR spectrometer (Bruker BioSpin SA, Fallanden, Switzerland) by comparing the signal with a ^{13}C pyruvate reference sample of a known concentration. The animals blood volume was calculated using the relation between total blood volume and body weight published by Lee and Blaufox [32] and the blood [1-^{13}C]acetate concentration was obtained accordingly.

The *in vitro* spin-lattice relaxation times of [1-^{13}C]acetylcarnitine were also measured at 400 MHz in D_2O and in freshly collected rat blood at 37° C using a saturation recovery sequence with proton decoupling during acquisition.

A non-linear least-squares quantification algorithm, AMARES, as implemented in the jMRUI software package [33], was used to fit the ^{13}C NMR data. The spectra were corrected for the phases and DC offset. Soft constraints were imposed to peak frequencies (182.55–182.65 ppm for acetate and 173.85–173.95 ppm for acetylcarnitine) and line widths (FWHM = 5–30 Hz) and the relative phases were fixed to zero. The acetylcarnitine peak areas were normalized to the maximum acetate signal in each experiment to account for varying polarization levels across experiments. The time courses of quantified peak areas were analyzed with the kinetic model described below, implemented in Matlab (The MathWorks, Natick, MA, USA).

2.1. Kinetic model of acetate metabolism

The uptake of acetate by skeletal muscle tissue as a function of the arterial concentration is described in [17,18]. Acetate transport across the cellular membrane occurs by facilitated diffusion, and thus net transport of acetate between the plasma and the tissue depends on the concentration gradient. We therefore assumed that the measured kinetic parameters are independent of processes related to membrane transport. As a result, the variations in conversion rates as a function of the injected concentration are expected to be directly correlated to ACS and CAT activity.

In the simplest model of a biochemical reaction, the conversion from substrate to product in a tissue can be described with a rate constant k that depends on substrate and enzyme concentrations. The assumption is that the enzyme concentration is not influenced by the substrate in the short time scale of the experiment, which is about 1 min. Therefore, the ^{13}C (*) label flow between the substrate acetate (Ace) and the metabolites acetylCoA (A.CoA) and acetylcarnitine (A.Car) in the skeletal muscle can be described as follows:

$$\frac{d[Ace^*]}{dt} = -V_{ACS}\frac{[Ace^*]}{[Ace]} \tag{1}$$

$$\frac{d[A.CoA^*]}{dt} = V_{ACS}\frac{[Ace^*]}{[Ace]} - V^f_{CAT}\frac{[A.CoA^*]}{[A.CoA]} + V^b_{CAT}\frac{[A.Car^*]}{[A.Car]} \tag{2}$$

$$\frac{d[A.Car^*]}{dt} = V^f_{CAT}\frac{[A.CoA^*]}{[A.CoA]} - \left(V^b_{CAT} + V_{OUT}\right)\frac{[A.Car^*]}{[A.Car]} \tag{3}$$

where $[Ace]$, $[A.CoA]$, $[A.Car]$ represent total metabolites concentrations (sum of ^{13}C labeled and unlabeled molecules), $[Ace^*]$, $[A.CoA^*]$, $[A.Car^*]$ the ^{13}C labeled concentrations, V^f_{CAT} and V^b_{CAT} are the forward and the backward fluxes through CAT, respectively, V_{ACS} is the flux through ACS and V_{OUT} is the flux out of the acetylcarnitine pool (Fig. 1). Since the physiological plasma acetate concentration is lower than 0.2 mM [5], it can be assumed that the acetate blood pool was fully labeled following the bolus injection, i.e. $[Ace^*]/[Ace] \approx 1$. Summing Eqs. (2) and (3) leads to:

$$\frac{d[A.Car^*]}{dt} + \frac{d[A.CoA^*]}{dt} = V_{ACS} - V_{OUT}\frac{[A.Car^*]}{[A.Car]} \tag{4}$$

The acetylCoA pool size is well regulated and is typically more than 10 times smaller than the acetylcarnitine pool [14], i.e. a small pool approximation [34,35] can be used, therefore $d[AcetylCoA^*]/dt \ll d[Acetylcarnitine^*]/dt$. The last term in Eq. (4) can be neglected since, within the short experimental time frame, the acetylcarnitine pool is only partially labelled and thus a minute amount of ^{13}C label will reach the mitochondrial acetylCoA pool. This is further supported by a previous study showing that the contribution of acetate to the TCA cycle in skeletal muscle was an order of magnitude smaller than our observed rate of acetylcarnitine formation [36,37]. Condensing the previous statements, the ^{13}C flow from acetate to acetylcarnitine in the skeletal muscle can be described by the following two equations:

$$\frac{d[Ace^*]}{dt} = -V_{ACS} = -k_{ACS}[Ace^*](t) \tag{5}$$

$$\frac{d[A.Car^*]}{dt} = V_{ACS} = k_{ACS}[Ace^*](t) \tag{6}$$

where the kinetic rate constant of ACS is introduced. Based on these conditions, it was concluded that the observed kinetic rate in these experiments corresponds to the enzymatic activity of ACS.

The acetate ^{13}C NMR signal measured in skeletal muscle tissue following the injection of hyperpolarized [1-^{13}C]acetate decayed with time as a consequence of a combination of (a) the loss of spin polarization related to longitudinal relaxation and characterized by an exponential decay rate R_1, (b) the loss of longitudinal magnetization due to radiofrequency excitations, and (c) the conversion of acetate into acetylcarnitine characterized by the kinetic rate constant k_{ACS}. The acetylcarnitine signal also decays because of (a) and (b), but (c) leads to an increase in signal. The time evolution of the carbonyl ^{13}C longitudinal magnetization of acetate, M_A, and acetylcarnitine, M_C, can thus be written as:

$$\frac{dM_A}{dt} = -R_A\left[M_A - M_{A,eq}\right] - k_{ACS}M_A \tag{7}$$

$$\frac{dM_C}{dt} = k_{ACS}M_A - R_{1,C}\left[M_C - M_{C,eq}\right] \tag{8}$$

where R_A, is the acetate signal decay comprising the carbonyl ^{13}C longitudinal relaxation rate $R_{1,A}$ as well as the potential [1-^{13}C]acetate flow of signal in and out of the volume of interest; $R_{1,C}$ is the carbonyl ^{13}C longitudinal relaxation rate of acetylcarnitine: Finally, $M_{A,eq}$ and $M_{C,eq}$ are the thermal equilibrium magnetizations of the carbonyl sites of acetate and acetylcarnitine, respectively. The contributions of $M_{A,eq}$ and $M_{C,eq}$ to the acetate and acetylcarnitine signals can be neglected since $M_A \gg M_{A,eq}$ and $M_C \gg M_{C,eq}$ when the resonances are detectable. These Bloch-McConnell differential equations [38] are identical to the ones derived for the one-compartment non steady-state metabolic model for one site exchange, which has already been shown to be applicable to hyperpolarized substrates [39]. From the initial conditions $M_C\ (t = 0) = 0$ and $M_A\ (t = 0) = M_0$ and taking into account the signal losses due to RF excitations, the hyperpolarized acetate and acetylcarnitine signals, $S_A(t)$ and $S_C(t)$, measured at $t = nT_R$, T_R being the repetition time, are given by:

$$S_A(t) \propto M_A(t)(\cos\theta)^{t/T_R} = M_0 e^{(-k_{ACS}-R_A)t}(\cos\theta)^{t/T_R} \tag{9}$$

$$S_C(t) \propto M_C(t)(\cos\theta)^{t/T_R} = M_0\left(be^{(-k_{ACS}-R_A)t} - be^{-R_{1,C}t}\right)(\cos\theta)^{t/T_R} \tag{10}$$

where $b = k_{ACS}/(-k_{ACS} - R_A + R_{1,C})$, and θ is the RF pulse flip angle. The time point of the first acetate observation, which also corresponds to the maximum acetate signal, was set to t = 0 prior to fitting the data with the kinetic model. To relate the signals measured in the sensitive volume of the surface coil described by Eqs. (9) and (10) to the cellular concentrations described by Eqs. (4) and (5), it was assumed that the blood volume in the VOI was small enough to neglect its contribution to the measured 13C acetate signal. This was supported by anatomical proton images taken prior to the injections and previous PET studies which determined a small blood volume in this area [40]. This assumption is strengthened by a reported acetate removal of 50% by skeletal muscle in a single passage of blood [5].

The dependence of the reaction kinetics on the hyperpolarized substrate concentration was analyzed using the standard Michaelis–

Menten equation, $v_{0,ACS} = V_{max} \cdot [Ace]/(K_M + [Ace])$ where K_M and V_{max} are the Michaelis constant and the initial reaction rate v_0 is the product of the initial acetate concentration and the kinetic rate constant, i.e., $v_{0,ACS} = k_{ACS} \cdot [Ace]$.

It has been observed that there exists a linear relationship between the kinetic rate constants obtained using mathematical modelling and the ratio of the areas of acetylcarnitine and acetate, a linearity also observed in studies using hyperpolarized pyruvate [41]. This linearity in case of hyperpolarized acetate was investigated by analysing the system of coupled equations defined by Eqs. (9) and (10) which has only 3 free parameters, namely k_{ACS}, R_A and $R_{1,C}$. It is possible to eliminate R_A by integrating the two equations over time and by taking their relative ratio as described in the Appendix A, yielding the following relationship:

$$k_{ACS} = R_{1,C}\frac{\int_0^\infty M_C(t)dt}{\int_0^\infty M_A(t)dt} \cong R_{1,C}\frac{\sum_{n=1}^{N} S_C((n-1)T_R)/\cos\theta^{(n-1)}}{\sum_{n=1}^{N} S_A((n-1)T_R)/\cos\theta^{(n-1)}} \quad (11)$$

where $S_C(nT_R)$ and $S_A(nT_R)$ are the signal intensity obtained at the nth of the N acquisitions, corrected for the loss of signal due to the RF pulses for acetylcarnitine and acetate, respectively, by the term $\cos\theta^{(n-1)}$.

3. Results

The incorporation of hyperpolarized ^{13}C label into acetylcarnitine was detected in all animals (n = 19). The average line width of the acetate resonance at 182.6 ppm was 21 ± 6 Hz and that of the acetylcarnitine resonance at 173.9 ppm was 6 ± 1 Hz (Fig. 2). The first acetate signal measured corresponds to the maximum observed signal which appeared 13.5 ± 2.3 s after the beginning of the injection and no progressive build-up of the signal was observed. The maximum acetylcarnitine signal was detected at a later time, 26.2 ± 3.9 s after the beginning of the injection. The maximal SNR of acetylcarnitine was 10 with zero line broadening and we imposed a minimum SNR threshold of 3 below which the signal was not taken into account for data analysis. In each experiment 1.0 mL of hyperpolarized acetate solution, with a concentration ranging from 40 to 290 mM was injected into the femoral vein. It was estimated that the injected hyperpolarized acetate doses resulted in a plasma acetate concentration ranging from 1.8 to 15.0 mM [32]. Using a previously reported relation between plasma and tissue acetate concentration in rat skeletal muscle [17], it was estimated that the tissue acetate concentration ranged from 0.12 to 1 mM.

Table 1
Longitudinal relaxation times of [1-^{13}C]acetylcarnitine at a magnetic field strength of 9.4 T in plasma and D_2O.

Solvent	T_1 in seconds
Blood T = 310 K (37 C)	14.9 ± 0.7
D_2O T = 295 K	10.3 ± 0.4
D_2O T = 305 K	14.3 ± 0.5
D_2O T = 310 K	15.5 ± 0.5

To determine k_{ACS} from the system of coupled equations defined by Eqs. (7) and (8), the longitudinal relaxation time of [1-^{13}C] acetylcarnitine was set to its *in vitro* value at 9.4 T, $T_{1,C} = 1/R_{1,C}$, of 14.9 ± 0.7 s determined in blood at physiological temperature (310 K, 37°C) (Table 1). The T_1 of acetylcarnitine in D_2O had a value similar to the T_1 in plasma at 310 K. Its T_1 decreases with decreasing temperature (Table 1). The kinetic rate constant k_{ACS} was determined by fitting Eqs. (9) and (10) to the time evolution of the acetate and acetylcarnitine signal integrals (Fig. 3) yielding k_{ACS} and R_A. The observed decay of the acetate signal is mono exponential with a time constant of 16.2 ± 1.4 s. The values of k_{ACS} were determined as a function of the tissue acetate concentration deduced from the infused acetate dose and the animal weight (Fig. 4). Yielding the initial reaction rates $v_{0,ACS} = k_{ACS} \cdot [Ace]$ as a function of the tissue acetate concentration, used to derive the Michaelis–Menten kinetic parameters (Fig. 4): The conversion of acetate into acetylcarnitine was characterized by a Michaelis constant K_M =

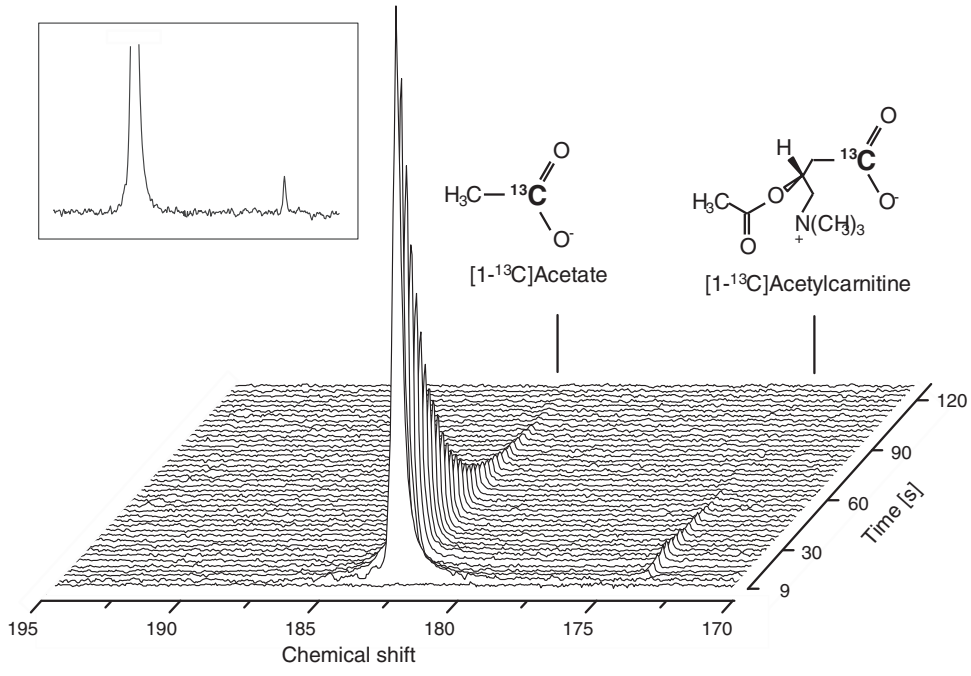

Fig. 2. Transient ^{13}C NMR spectra of hyperpolarized acetate (182.6 ppm) and its metabolic product acetylcarnitine (173.9 ppm) in healthy skeletal muscle *in vivo*. The transfer of the ^{13}C label is catalyzed by the enzymes ACS and CAT. Spectra were acquired every 3 s using adiabatic 30° excitation pulses and ^{1}H decoupling during acquisition, a 1.0 mL solution of a 110 mM hyperpolarized acetate was injected. Inset: summation of the spectra as described in Eq. (11) which was used to calculate the kinetic rate constants.

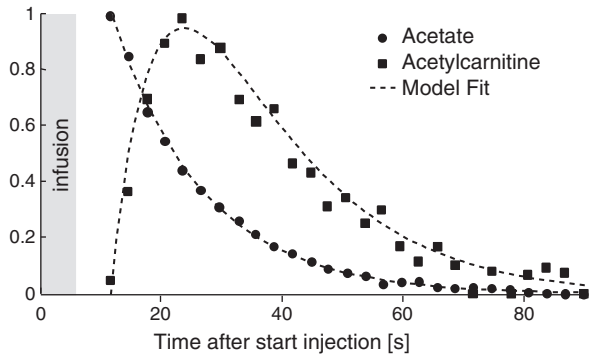

Fig. 3. Time course of the normalized peak integrals of hyperpolarized acetate (●) and its metabolic product acetylcarnitine (■). The kinetic model described with Eqs. (9) and (10) was used to fit (- - -) the hyperpolarized time courses to determine the kinetic rate constant k_{ACS}, and the decay rate of acetate R_A. The time courses were normalized to their maximum signal. In the data shown here 1.0 mL of a 110 mM hyperpolarized acetate solution was injected.

0.35 ± 0.13 mM, as obtained with the model and a maximal reaction rate, V_{max}, of 0.199 ± 0.031 μmol/g/min. The summation approach estimated a K_M = 0.32 ± 0.12 mM and V_{max}, of 0.190 ± 0.029 μmol/g/min.

To further demonstrate that the kinetic rate constant is uniquely determined when the relaxation rate of acetylcarnitine $R_{1,C}$ is fixed, k_{ACS} was calculated for all experiments using Eq. (11) and plotted against the kinetic rate constants obtained from the fitting procedure (Fig. 5). The residual differences are most likely due to the fitting errors inherent to the limited signal-to-noise ratio.

4. Discussion

The present study demonstrates that kinetic rates for the conversion of acetate to acetylcarnitine can be derived from *in vivo* hyperpolarized magnetic resonance experiments and that these rates are in very good agreement with the ones determined in *in vitro* experiments. The plasma acetate concentrations used in the current study (1.8–15.1 mM) have been previously shown to linearly scale with the uptake of acetate in skeletal muscle tissue and thus with the cellular acetate concentration [17,18]. This implies that the kinetic parameters extracted from the *in vivo* real-time measurements presented herein are independent of processes related to membrane transport since acetate uptake by resting skeletal muscle is proportional to the arterial concentration. Therefore, the variations in conversion rates as a function of the injected concentration are thus directly correlated to the biochemical transformations regulated by ACS and CAT in the cytosol. CAT also resides in the mitochondria where it converts acetylcarnitine back into acetylCoA followed by entry into the TCA cycle and ^{13}C MRS cannot distinguish between the two compartments. However, since compared to other substrates there is a relatively small (~3%) contribution of acetate to mitochondrial acetylCoA in the skeletal muscle [36,37], and in addition the cytosolic acetylcarnitine pool is only partially labelled during the short duration of the experiments, it is expected that the [1-^{13}C] acetylcarnitine signal almost exclusively originates from the cytosol.

The tissue concentrations used in the present study (0.12–1.00 mM) were approximately an order of magnitude lower than those used to maximally acetylate free carnitine and CoA in canine skeletal muscle [15] and human skeletal muscle at rest [42–44]. This indicates that the observed acetylcarnitine formation was not hindered

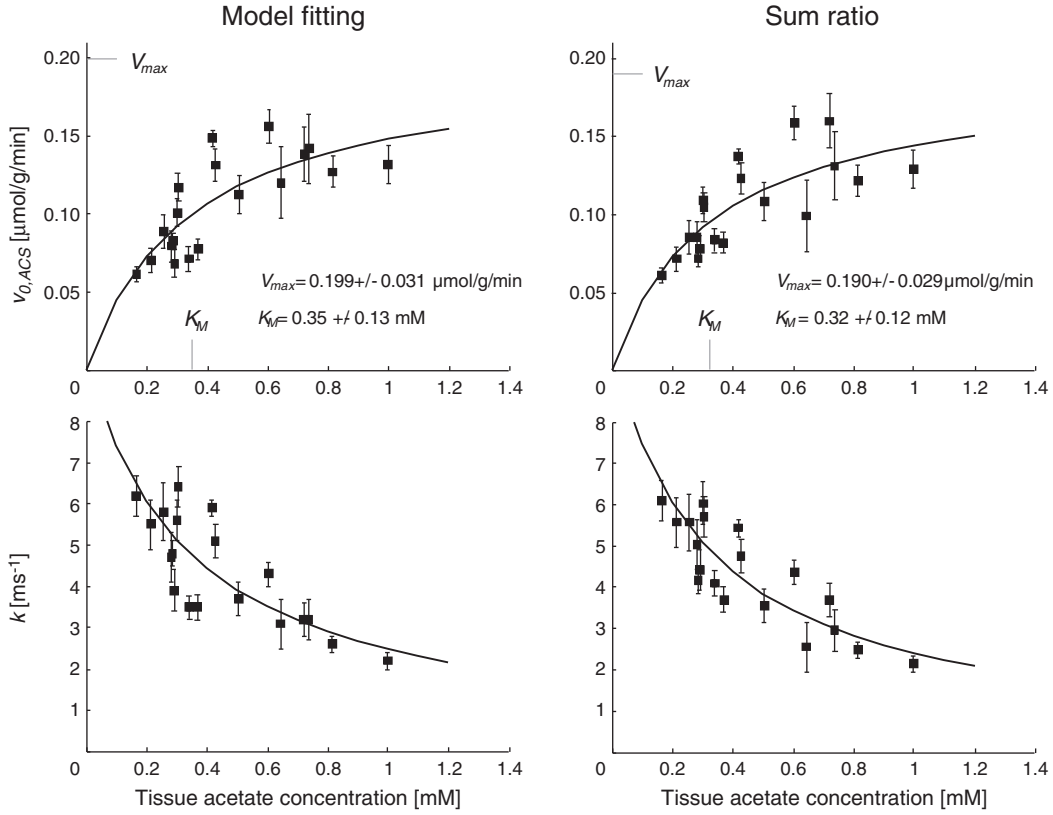

Fig. 4. The relation between the initial reaction rates $v_{0,ACS}$ (top row) and kinetic rate constants k_{ACS} (bottom row) with the hyperpolarized [1-^{13}C]acetate concentration. Every hyperpolarized experiment provided one kinetic rate constant k_{ACS} (■) and associated standard deviation as derived from the fit to the kinetic model (left column) or using the summation approach (right column). The initial reaction rate was obtained by multiplying the fitted kinetic rate constant k_{ACS} with the corresponding substrate concentration. Michaelis–Menten parameter fits are represented by the dashed line. Using model fitting a K_M of 0.35 ± 0.13 mM and V_{max} of 0.199 ± 0.031 μmol/g/min were estimated. Using the summation approach a K_M of 0.32 ± 0.12 mM and V_{max} of 0.190 ± 0.029 μmol/g/min was obtained.

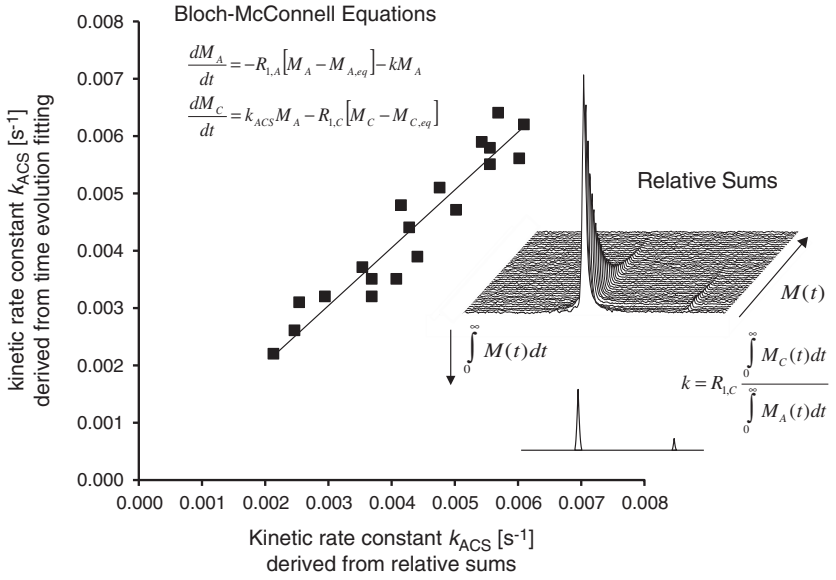

Fig. 5. The linear relationship between the kinetic rate constants k_{ACS} obtained with mathematical modeling of the metabolite time courses and the ratio of the sum of RF corrected peak integrals of acetylcarnitine ($C(t)$) and acetate ($A(t)$) was used to calculate an integral derived kinetic rate constant (Eq. (11)). The integral derived kinetic rate constant equals the integral ratio times the longitudinal relaxation rate of acetylcarnitine $R_{1,C}$. The relationship between the kinetic rate constants derived from the metabolic model versus the kinetic rate constants derived using the relative areas of hyperpolarized acetylcarnitine and acetate are shown below.

by a decrease in carnitine availability to CAT. The observed kinetic rate constants range from ~2 to 6 ms^{-1}, showing that substrate concentration is an important parameter to take into account while designing a study using hyperpolarized acetate as a metabolic tracer. It was also observed that this conversion is not saturated even at a tissue concentration of acetate as high as 1 mM.

Our analysis based on the assumption that, during the experimental time frame, the acetate pool is fully labeled and the time variation of the acetylCoA pool labeling is much smaller than the one of acetylcarnitine led to the conclusion that the kinetic rates corresponds to the conversion rate associated with the enzyme acetylCoA synthetase. This is further supported by the fact that the transformation catalyzed by ACS is the rate-limiting step in the transformation of acetate into acetylcarnitine [4]. It needs to be mentioned that the reaction through ACS is irreversible and there is no direct exchange between acetate and acetylcarnitine. Previous reported ACS activity suggested an in vitro K_M of 0.2 mM for acetate [20]. Following acetate infusions in rat and sheep, the Michaelis constant for acetate in the ACS reaction was between 0.28 and 0.39 mM, based on tissue extracts, with no marked differences between species, tissue or the intracellular location of the enzyme activity [5]. These values of K_M are in agreement with our observed Michaelis constant.

Based on the linear relationship between the ratio of signal integrals and the kinetic rate constants, two approaches were used to extract k_{ACS} from the data: One was based on time evolution fitting of the signal integrals (Eqs. (9) and (10)) and the other on the relative ratio of the sum of both substrate and product (Eq. (11)). Note that, while the first requires the use of mathematical modeling, the summation approach is simpler but less accurate because each individual spectrum has to be divided by a factor of cos $\theta^{(n-1)}$ according to Eq. (11), where n is the acquisition number, leading to noise error propagation, whereas the fit of the time series takes into account the RF decay and only relies on raw data. Other approaches based on mathematical modeling of the metabolic time course were previously proposed to determine the conversion rates from hyperpolarized ^{13}C-labeled pyruvate to its downstream metabolites [39,45,46].

Acetylcarnitine ^{13}C labeling in the heart has been previously reported following the infusion of hyperpolarized [2-^{13}C]pyruvate [26,27], but unlike pyruvate, acetate is independent of PDH flux. The utilization of acetate by the TCA cycle is strictly aerobic and depending on the delivery of both acetate and oxygen [5], the conversion rate constants are expected to be strongly dependent on the oxygenation of the tissue under investigation and TCA cycle activity: It was previously shown that intense muscle activity lead to an accumulation of acetylcarnitine [11], and that a decreased exchange between acetylcarnitine and acetate was a relevant marker for ischemia [25]. The possibility to monitor the acetylcarnitine kinetics *in vivo* in a measurement window of 1 min in a non-invasive manner and the extraction of specific enzymatic activities can be expected to be a valuable tool for differentiating between healthy and pathological metabolism, in particular since the conversion rate regulated by ACS is implicated in disorders like diabetes [47] or cancer [48].

5. Conclusions

The conversion rates from hyperpolarized acetate into acetylcarnitine can be quantified *in vivo*, and although separated by two enzymatic reactions, these rates define uniquely the activity of acetylCoA synthetase. It was further shown that these rates can be obtained using either fitting of time courses, or an analysis based on time course integration, both approaches yielded similar enzymatic activity. This study showed the feasibility of measuring the activity of acetylCoA synthetase *in vivo*.

Conflict of interest

The authors declare that they have no conflict of interest.

Acknowledgements

We thank Hanne Frenkel, Jacquelina Romero, Laure Bardouillet and Mario Lepore for veterinary support, Christine Nabuurs, Bernard Lanz and Costas Anastassiou for helpful discussions, and Christophe Roussel for his insights about biochemical analysis. This work was supported by the Swiss National Science Foundation (PP00P2_133562 and 31003A_131087), the National Competence Center in Biomedical

Imaging (NCCBI), the Centre d'Imagerie BioMédicale (CIBM) of the UNIL, UNIGE, HUG, CHUV, EPFL, and the Leenaards and Jeantet Foundations.

Appendix A

Derivation of Eqs. (11) from (9) and (10)

The transient magnetization of hyperpolarized acetate and its metabolic product acetylcarnitine can be described as follows:

$$M_A(t) = M_0 e^{(-k_{ACS}-R_A)t}$$
$$M_C(t) = M_0\left(be^{(-k_{ACS}-R_A)t} - be^{-R_{1,C}t}\right)$$

With $b = k_{ACS}/(-k_{ACS} - R_A + R_{1,C})$. Integration of both equations from t = 0 to infinity results in the following

$$\int_0^\infty M_A(t)dt = M_0\int_0^\infty e^{(-k_{ACS}-R_A)t}dt = M_0\frac{e^{(-k_{ACS}-R_A)t}}{(-k_{ACS}-R_A)}\Big|_0^\infty = -\frac{M_0}{k_{ACS}+R_A}$$

$$\int_0^\infty M_C(t)dt = bM_0\int_0^\infty e^{(-k_{ACS}-R_A)t}dt - bM_0\int_0^\infty e^{-R_{1,C}t}dt = -\frac{M_0 b}{k_{ACS}+R_A} + \frac{M_0 b}{R_{1,C}}$$

$$\frac{\int_0^\infty M_C(t)dt}{\int_0^\infty M_A(t)dt} = \frac{-\frac{M_0 b}{k_{ACS}+R_A} + \frac{M_0 b}{R_{1,C}}}{-\frac{M_0}{k_{ACS}+R_A}} = b\left(1 - \frac{k_{ACS}}{R_{1,C}} - \frac{R_A}{R_{1,C}}\right) =$$

$$\frac{\int_0^\infty M_C(t)dt}{\int_0^\infty M_A(t)dt} = \left(\frac{k_{ACS}}{-k_{ACS}-R_A+R_{1,C}}\right)\left(\frac{-k_{ACS}-R_A+R_{1,C}}{R_{1,C}}\right) = \frac{k_{ACS}}{R_{1,C}}$$

$$k_{ACS} = R_{1,C}\frac{\int_0^\infty M_C(t)dt}{\int_0^\infty M_A(t)dt} \cong R_{1,C}\frac{\sum_{n=1}^{N} S_C((n-1)TR)/\cos\theta^{(n-1)}}{\sum_{n=1}^{N} S_A((n-1)TR)/\cos\theta^{(n-1)}}$$

References

[1] E.N. Bergman, Energy contributions of volatile fatty acids from the gastrointestinal tract in various species, Physiol. Rev. 70 (1990) 567–590.
[2] E.D. Mayfield, A. Bensadoun, B.C. Johnson, Acetate metabolism in ruminant tissues, J. Nutr. 89 (1966) 189–196.
[3] P. Vinay, M. Prud'Homme, B. Vinet, G. Cournoyer, P. Degoulet, M. Leville, A. Gougoux, G. St-Louis, L. Lapierre, Y. Piette, Acetate metabolism and bicarbonate generation during hemodialysis: 10 years of observation, Kidney Int. 31 (1987) 1194–1204.
[4] C. Barth, M. Sladek, K. Decker, Dietary changes of cytoplasmic acetyl-coa synthetase in different rat tissues, Biochim. Biophys. Acta 260 (1972) 1–9.
[5] S.E. Knowles, I.G. Jarrett, O.H. Filsell, F.J. Ballard, Production and utilization of acetate in mammals, Biochem. J. 142 (1974) 401–411.
[6] P.M.L. Robitaille, D.P. Rath, A.M. Abduljalil, J.M. Odonnell, Z.C. Jiang, H.Z. Zhang, R.L. Hamlin, Dynamic C-13 Nmr analysis of oxidative-metabolism in the in-vivo canine myocardium, J. Biol. Chem. 268 (1993) 26296–26301.
[7] H. Sone, L. Shimano, N. Inoue, Y. Sakakura, M. Amemiya, A. Takahashi, M. Osawa, A. Iwama, N. Yamada, Acetyl-coenzyme a synthetase is a new lipogenic enzyme controlled by sterol regulatory element-finding proteins and influenced by diabetes, Diabetes 50 (2001) A407-A407.
[8] I.B. Fritz, S.K. Schultz, P.A. Srere, Properties of partially purified carnitine acetyltransferase, J. Biol. Chem. 238 (1963) 2509–2517.
[9] A.L. Carter, D.L. Lennon, F.W. Stratman, Increased acetyl carnitine in rat skeletal muscle as a result of high-intensity short-duration exercise. Implications in the control of pyruvate dehydrogenase activity, FEBS Lett. 126 (1981) 21–24.
[10] C.C. Childress, B. Sacktor, D.R. Traynor, Function of carnitine in the fatty acid oxidase-deficient insect flight muscle, J. Biol. Chem. 242 (1967) 754–760.
[11] F.B. Stephens, D. Constantin-Teodosiu, P.L. Greenhaff, New insights concerning the role of carnitine in the regulation of fuel metabolism in skeletal muscle, J. Physiol. 581 (2007) 431–444.
[12] R.R. Ramsay, V.A. Zammit, Carnitine acyltransferases and their influence on CoA pools in health and disease, Mol. Aspects Med. 25 (2004) 475–493.
[13] J. Bremer, Carnitine—metabolism and functions, Physiol. Rev. 63 (1983) 1420–1480.
[14] L.L. Spriet, D.J. Dyck, G. Cederblad, E. Hultman, Effects of fat availability on acetyl-CoA and acetylcarnitine metabolism in rat skeletal muscle, Am. J. Physiol. 263 (1992) C653–C659.
[15] P.A. Roberts, S.J.G. Loxham, S.M. Poucher, D. Constantin-Teodosiu, P.L. Greenhaff, Acetyl-CoA provision and the acetyl group deficit at the onset of contraction in ischemic canine skeletal muscle, Am. J. Physiol. Endocrinol. Metab. 288 (2005) E327–E334.
[16] E. Ciaranfi, A. Fonnesu, Time-course of injected acetate in normal and depancreatized dogs, Biochem. J. 57 (1954) 171–175.
[17] N. Karlsson, E. Fellenius, K.H. Kiessling, The metabolism of acetate in the perfused hind-quarter of the rat, Acta Physiol. Scand. 93 (1975) 391–400.
[18] B. Mittendorfer, L.S. Sidossis, E. Walser, D.L. Chinkes, R.R. Wolfe, Regional acetate kinetics and oxidation in human volunteers, Am. J. Physiol. Endocrinol. Metab. 274 (1998) E978–E983.
[19] L.A. Bertocci, J.G. Jones, C.R. Malloy, R.G. Victor, G.D. Thomas, Oxidation of lactate and acetate in rat skeletal muscle: Analysis by C-13-nuclear magnetic resonance spectroscopy, J. Appl. Physiol. 83 (1997) 32–39.
[20] L.T. Webster Jr., [58] Acetyl-CoA synthetase, in: M.L. John (Ed.), Method Enzymol, Academic Press, 1969, pp. 375–381.
[21] R. Gruetter, In vivo C-13 NMR studies of compartmentalized cerebral carbohydrate metabolism, Neurochem. Int. 41 (2002) 143–154.
[22] J.H. Ardenkjaer-Larsen, B. Fridlund, A. Gram, G. Hansson, L. Hansson, M.H. Lerche, R. Servin, M. Thaning, K. Golman, Increase in signal-to-noise ratio of >10,000 times in liquid-state NMR, Proc. Natl. Acad. Sci. U.S.A. 100 (2003) 10158–10163.
[23] K. Golman, R. in't Zandt, M. Thaning, Real-time metabolic imaging, Proc. Natl. Acad. Sci. U.S.A. 103 (2006) 11270–11275.
[24] J. Kurhanewicz, D.B. Vigneron, K. Brindle, E.Y. Chekmenev, A. Comment, C.H. Cunningham, R.J. DeBerardinis, G.G. Green, M.O. Leach, S.S. Rajan, R.R. Rizi, B.D. Ross, W.S. Warren, C.R. Malloy, Analysis of cancer metabolism by imaging hyperpolarized nuclei: prospects for translation to clinical research, Neoplasia 13 (2011) 81–97.
[25] P.R. Jensen, T. Peitersen, M. Karlsson, R. In 't Zandt, A. Gisselsson, G. Hansson, S. Meier, M.H. Lerche, Tissue-specific short chain fatty acid metabolism and slow metabolic recovery after ischemia from hyperpolarized NMR in vivo, J. Biol. Chem. 284 (2009) 36077–36082.
[26] H.J. Atherton, M.S. Dodd, L.C. Heather, M.A. Schroeder, J.L. Griffin, G.K. Radda, K. Clarke, D.J. Tyler, Role of pyruvate dehydrogenase inhibition in the development of hypertrophy in the hyperthyroid rat heart a combined magnetic resonance imaging and hyperpolarized magnetic resonance spectroscopy study, Circulation 123 (2011), (2552-U2134).
[27] M.A. Schroeder, H.J. Atherton, M.S. Dodd, P. Lee, L.E. Cochlin, G.K. Radda, K. Clarke, D.J. Tyler, The cycling of acetyl-coenzyme A through acetylcarnitine buffers cardiac substrate supply: a hyperpolarized 13C magnetic resonance study, Circ. Cardiovasc. Imaging 5 (2012) 201–209.
[28] A. Comment, B. van den Brandt, K. Uffmann, F. Kurdzesau, S. Jannin, J.A. Konter, P. Hautle, W.T. Wenckebach, R. Gruetter, J.J. van der Klink, Design and performance of a DNP prepolarizer coupled to a rodent MRI scanner, Concepts Magn. Reson. Part B: Magn. Reson. Eng. 31B (2007) 255–269.
[29] S. Jannin, A. Comment, F. Kurdzesau, J.A. Konter, P. Hautle, B. van den Brandt, J.J. van der Klink, A 140 GHz prepolarizer for dissolution dynamic nuclear polarization, J. Chem. Phys. 128 (2008) 241102.
[30] T. Cheng, M. Mishkovsky, J.A.M. Bastiaansen, O. Ouari, P. Hautle, P. Tordo, B.v.d. Brandt, A. Comment, Method to minimize and monitor in situ the polarization losses in hyperpolarized biomolecules prior to in vivo MR experiments. 2013 (in press).
[31] R. Gruetter, I. Tkac, Field mapping without reference scan using asymmetric echo-planar techniques, Magn. Reson. Med. 43 (2000) 319–323.
[32] H.B. Lee, M.D. Blaufox, Blood volume in the rat, J. Nucl. Med. 26 (1985) 72–76.
[33] A. Naressi, C. Couturier, J.M. Devos, M. Janssen, C. Mangeat, R. de Beer, D. Graveron-Demilly, Java-based graphical user interface for the MRUI quantitation package, MAGMA 12 (2001) 141–152.
[34] K. Uffmann, R. Gruetter, Mathematical modeling of C-13 label incorporation of the TCA cycle: the concept of composite precursor function, J. Neurosci. Res. 85 (2007) 3304–3317.
[35] J.M.N. Duarte, B. Lanz, R. Gruetter, Compartmentalised cerebral metabolism of [1,6-13C]glucose determined by in vivo 13C NMR spectroscopy at 14.1 T, Front. Neuroenerg. 3 (2011).
[36] D.E. Befroy, K.F. Petersen, S. Dufour, G.F. Mason, R.A. de Graaf, D.L. Rothman, G.I. Shulman, Impaired mitochondrial substrate oxidation in muscle of insulin-resistant offspring of type 2 diabetic patients, Diabetes 56 (2007) 1376–1381.
[37] D.E. Befroy, K.F. Petersen, S. Dufour, G.F. Mason, D.L. Rothman, G.I. Shulman, Increased substrate oxidation and mitochondrial uncoupling in skeletal muscle of endurance-trained individuals, Proc. Natl. Acad. Sci. U.S.A. 105 (2008) 16701–16706.
[38] H.M. Mcconnell, Reaction rates by nuclear magnetic resonance, J. Chem. Phys. 28 (1958) 430–431.
[39] S.E. Day, M.I. Kettunen, F.A. Gallagher, D.E. Hu, M. Lerche, J. Wolber, K. Golman, J.H. Ardenkjaer-Larsen, K.M. Brindle, Detecting tumor response to treatment using hyperpolarized (13)C magnetic resonance imaging and spectroscopy, Nat. Med. 13 (2007) 1382–1387.

[40] M. Mizuno, Y. Kimura, T. Iwakawa, K. Oda, K. Ishii, K. Ishiwata, Y. Nakamura, I. Muraoka, Regional differences in blood volume and blood transit time in resting skeletal muscle, Jpn. J. Physiol. 53 (2003) 467–470.
[41] Deborah K. Hill, E. Mariotti, M.R. Orton, J.K.R. Boult, Y. Jamin, S.P. Robinson, N.M.S. Al-Saffar, M.O. Leach, Yuen-Li Chung, T.R. Eykyn, Model free approach to kinetic analysis of real-time hyperpolarised 13C MRS data, Proc. Int. Soc. Magn. Reson. Med. 20 (2012) 1738, (Melbourne, Australia).
[42] M.K. Evans, I. Savasi, G.J.F. Heigenhauser, L.L. Spriet, Effects of acetate infusion and hyperoxia on muscle substrate phosphorylation after onset of moderate exercise, Am. J. Physiol. Endocrinol. Metab. 281 (2001) E1144–E1150.
[43] R.A. Howlett, G.J.F. Heigenhauser, L.L. Spriet, Skeletal muscle metabolism during high-intensity sprint exercise is unaffected by dichloroacetate or acetate infusion, J. Appl. Physiol. 87 (1999) 1747–1751.
[44] C.T. Putman, L.L. Spriet, E. Hultman, D.J. Dyck, G.J. Heigenhauser, Skeletal muscle pyruvate dehydrogenase activity during acetate infusion in humans, Am. J. Physiol. 268 (1995) E1007–E1017.
[45] M.L. Zierhut, Y.F. Yen, A.P. Chen, R. Bok, M.J. Albers, V. Zhang, J. Tropp, I. Park, D.B. Vigneron, J. Kurhanewicz, R.E. Hurd, S.J. Nelson, Kinetic modeling of hyperpolarized (13)C(1)-pyruvate metabolism in normal rats and TRAMP mice, J. Magn. Reson. 202 (2010) 85–92.
[46] T. Xu, D. Mayer, M. Gu, Y.F. Yen, S. Josan, J. Tropp, A. Pfefferbaum, R. Hurd, D. Spielman, Quantification of in vivo metabolic kinetics of hyperpolarized pyruvate in rat kidneys using dynamic C-13 MRSI, NMR Biomed. 24 (2011) 997–1005.
[47] M.S. Kornacke, J.M. Lowenste, Citrate and conversion of carbohydrate into fat—activities of citrate-cleavage enzyme and acetate thiokinase in livers of starved and re-fed rats, Biochem. J. 94 (1965) 209–215.
[48] Y. Yoshii, T. Furukawa, H. Yoshii, T. Mori, Y. Kiyono, A. Waki, M. Kobayashi, T. Tsujikawa, T. Kudo, H. Okazawa, Y. Yonekura, Y. Fujibayashi, Cytosolic acetyl-CoA synthetase affected tumor cell survival under hypoxia: the possible function in tumor acetyl-CoA/acetate metabolism, Cancer Sci. 100 (2009) 821–827.